2022 International Conference on Radar, Antenna, Microwave, Electronics, and Telecommunications (ICRAMET) | 978-1-6654-5412-4/22/$31.00 ©2022 IEEE | DOI: 10.1109/ICRAMET56917.2022.9991222

Webots-Based: Design of Collision Free Trajectory of Wheeled Mobile Robot Using Artificial Potential Field

Riky Dwi Puriyanto
Dept. of Electrical Engineering
Universitas Ahmad Dahlan
Yogyakarta, Indonesia
rikydp@ee.uad.ac.id

Ika Wulandari
Pusat Riset Teknologi Hidrodinamika
Badan Riset dan Inovasi Nasional
Surabaya, Indonesia
ikaw001@brin.go.id

Alfian Ma'arif
Dept. of Electrical Engineering
Universitas Ahmad Dahlan
Yogyakarta, Indonesia
alfianmaarif@ee.uad.ac.id

Haris Imam Karim Fathurrahman
Dept. of Electrical Engineering
Universitas Ahmad Dahlan
Yogyakarta, Indonesia
haris.fathurrahman@te.uad.ac.id

Phisca Aditya Rosyady
Dept. of Electrical Engineering
Universitas Ahmad Dahlan
Yogyakarta, Indonesia
phisca.aditya@te.uad.ac.id

***Abstract*—Wheeled mobile robot (WMR) is widely used in everyday life. The problem that arises in its implementation is navigation. Besides that, integrating navigation components, especially path planning, in a WMR kinematic model is considered very important to produce natural robot motion. One of the reliable path planning algorithms that can be used in real-time is Artificial Potential Field (APF). The weakness of this algorithm is that it can be stuck at the local minimum. Modification of APF (MAPF) which several researchers have proposed, serves to solve the drawbacks of this algorithm. This study aims to integrate and implement navigation capabilities in the WMR kinematics model, especially path planning. The test was carried out in a simulation using the Webots simulator. The robot used is an E-puck robot. E-puck is a differential drive mobile robot (DDMR) that uses two drivers to move. The results show that the MAPF path planning algorithm can be implemented well in the WMR kinematics model. Local minimum problems in the form of symmetrically aligned robot-obstacle-goal (SAROG) and goal non-reachable due to obstacle nearby (GNRON) in real conditions can be solved properly.**

***Index Terms*—mobile robot, path planning, APF, local minimum, kinematics model.**

I. Introduction

Autonomous mobile robot (AMR) is widely implemented in everyday life to help complete human work. Generally, AMR is used to do repetitive work and work in hazardous environments. One type of AMR widely used in daily life is a robot that moves with wheels or is commonly called a wheeled mobile robot (WMR). Robots with wheel drive are widely used because of human habits in using wheeled cars in everyday life. WMR is widely used in the fields of health [1], [2], education [3], [4], industry [5], [6], and agriculture [7], [8].

The main problem in implementing an autonomous WMR is its navigation capabilities. Navigation comprises several main components, such as localization, mapping, and path planning [9]. Localization is the robot's ability to find out the robot's position in real-time. One of the methods used to determine the robot's location is a motor encoder and gyroscope [10]. Mapping is the robot's ability to recognize the environment around the robot. In general, mapping can be done by embedding information in the robot's memory and building a map through sensors attached to the robot.

In addition to localization and mapping, path planning is one of the navigation capabilities considered important for WMR, which moves autonomously to produce a collision-free trajectory. A good path planning algorithm can reduce investment in terms of financial and robot development time [11], [12]. One of the path planning algorithms that has a simple equation but is considered reliable and is still used today is the Artificial Potential Field (APF) [13]–[16]. This algorithm utilizes the attractive potential field generated by the target to pull the robot closer to the target. In addition, this algorithm also utilizes the repulsive potential field from obstacles to push the robot away from obstacles.

A WMR can move naturally by utilizing the WMR kinematic model. However, the problem faced in autonomously moving WMR is how to avoid collisions. Therefore, it is necessary to integrate the WMR kinematics model with the path design algorithm. In addition, the design of the path of a WMR also requires information support in the form of the position of the robot and the conditions of the surrounding environment. The accuracy of the information provided by other navigation components will make an important contribution to designing the WMR path so that it can move autonomously.

Research on the implementation of the path design algo-

978-1-6654-5412-4/22/$31.00 ©2022 IEEE

rithm, especially APF on WMR, has been carried out. The test is generally done by modelling the robot as a moving point of mass in a test environment. Testing using a real robot model needs to be done to see the effect of the implementation of the APF algorithm on the robot's motion. However, real implementation requires a fairly high financial investment. Therefore, researchers mainly do testing using a simulator that shows a robot's real performance.

This study aims to integrate and implement the path planning algorithm on the WMR kinematics model. The performance evaluation of the APF pad WMR algorithm was carried out by simulation using the Webots simulator. The type of robot used is a robot with a different drive, or a differential drive mobile robot.

II. METHOD

A. Artificial Potential Field (APF) Algorithm

The Artificial Potential Field (APF) algorithm was introduced by Khatib [17] to create a trajectory on a robotic arm. The APF algorithm is considered a simple but reliable equation in real-time implementation. In the APF algorithm, the robot is considered as a point of mass in a potential field and then combines the attractive force from the target point as an attractive potential field and the repulsive potential field in the robot's working field to form a safe path. This algorithm is advantageous because the path traversed is based on quantitative calculations.

The APF algorithm is the same principle as the spring's potential energy (E_p) according to equation (1). The value of k is the spring constant, while the value of x is the spring strain from a stable condition. The spring's potential energy is the energy that causes the spring to return to its initial position after the force on the spring is removed. The energy released to pull the spring is stored in the spring, which is then referred to as the potential energy of the spring. The further the spring is stretched, the more potential energy is generated.

$$E_p = \frac{1}{2}k\Delta x^2 \tag{1}$$

The robot's position in an environment coordinates as $q = (x, y)$. The APF algorithm generates a potential field that is utilized by the robot to generate a safe path. The artificial potential field generated is based on the parameters of the robot's distance to the target (D_{rg}), the distance of the obstacle to the robot (D_{or}), and the robot's safe distance to the obstacle points/safe distance (r). The equation for the attractive and repulsive potential fields proposed by Khatib can be seen in (2) and (3).

$$U_a(q) = \frac{1}{2}k_a D_{rg}^2 \tag{2}$$

$$U_r(q) = \begin{cases} \frac{1}{2}k_r \left(\frac{1}{D_{or}} - \frac{1}{r}\right)^2 & \text{if } D_{or} \leq r \\ 0 & \text{if } D_{or} > r \end{cases} \tag{3}$$

The value of D_{rg} and D_{or} is an Euclidean distance which has the equation $\|q - q_g\|$ and $\|q_o - q\|$, with the target position $q_g = (x_g, y_g)$ and the obstacle $q_o = (x_o, y_o)$, respectively.

The problem in implementing the APF algorithm is that the robot can be trapped in the minimum local area. The known minimum local forms are symmetrically aligned robot-obstacle-goal (SAROG) and goal non-reachable due to nearby obstacle (GNRON) [14], [18]. The SAROG problem occurs when the robot, obstacle and target are in a straight line. This condition, in theory, will cause a deadlock condition when the robot is in the presence of obstacles. The GNRON problem occurs when the obstacle is very close to the target. This condition is indicated by the value of Drg, which is smaller than the safe distance. The minimum global position that should be in the target coordinates will be shifted due to obstacles located very close to the target.

Researcher [19] used modified APF (MAPF) to solve local minimum problems. The equation used is to replace equation (3) into (4).

$$U_r(q) = \begin{cases} \frac{1}{2}k_r \left(\frac{1}{D_{or}} - \frac{1}{r}\right)^2 D_{rg}^n & \text{if } D_{or} \leq r \\ 0 & \text{if } D_{or} > r \end{cases} \tag{4}$$

where n is the tuning parameter to solve the local minimum problem. The total potential field ($U_t(q)$) generated by the modified APF algorithm based on (2) and (4) can be seen in (5). The comparison of the total potential field of APF and modification of APF can be seen in Fig. 1.

$$U_t(q) = U_a(q) + U_r(q) \tag{5}$$

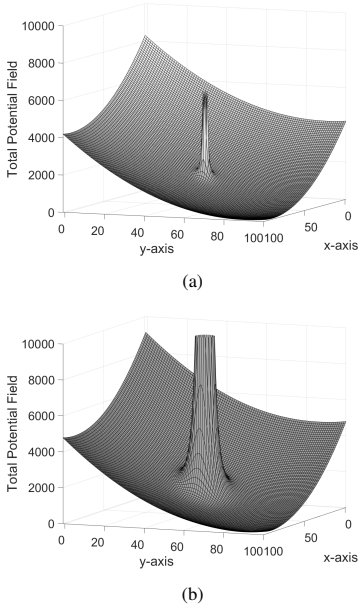

Fig. 1. Comparison of APF and MAPF total potential field (a) Potential field of APF path planning algorithm (b) Potential field of MAPF path planning algorithm

978-1-6654-5412-4/22/$31.00 ©2022 IEEE

The APF algorithm produces movement towards the target at the minimum potential field value. Therefore, a negative gradient of $U_t(q)$ is needed to direct the robot towards the equilibrium point at the goal point. The negative gradient of $U_t(q)$ is shown in equations (6) and (7).

$$F_x(q) = -k_\alpha(x - x_g) - k_r \frac{\left(\frac{1}{D_{or}} - \frac{1}{r}\right)(x_o - x)D_{rg}^n}{D_{or}^3} \\ -0.5k_r n \left(\frac{1}{D_{or}} - \frac{1}{r}\right)^2 (x - x_g)D_{rg}^{n-2} \tag{6}$$

$$F_y(q) = -k_\alpha(y - y_g) - k_r \frac{\left(\frac{1}{D_{or}} - \frac{1}{r}\right)(y_o - y)D_{rg}^n}{D_{or}^3} \\ -0.5k_r n \left(\frac{1}{D_{or}} - \frac{1}{r}\right)^2 (y - y_g)D_{rg}^{n-2} \tag{7}$$

where $F_x(q)$ and $F_y(q)$ are negative gradient of the total potential field in x and y axes.

B. Kinematics Model of Wheeled Mobile Robot (WMR)

This study will implement a potential field-based path planning algorithm in the WMR kinematics model. The WMR kinematics model is used because the test in this study will only use the speed component without involving the force or torque component that applies to the robot. WMR kinematic equation can be seen in (8).

$$\begin{aligned} \dot{x} &= v\ cos\ \theta \\ \dot{y} &= v\ sin\ \theta \\ \dot{\theta} &= \omega \end{aligned} \tag{8}$$

where v is linear velocity and ω is angular velocity.

Parameters affecting WMR motion can be seen in Fig. 2. Based on Fig. 2, the robot in the initial position $\{I\}$ has a heading angle (θ) which moves to the target $\{G\}$ at a distance of ρ. The angle that the robot makes to the robot's final position is defined as θ. The difference between the initial and the destination on each axis of the Cartesian coordinates is Δx and Δy. The robot heading angle to the initial robot frame is defined as β. In this study, the value of α is influenced by the negative gradient of the MAPF algorithm according to equation (9).

$$\begin{aligned} \rho &= \sqrt{\Delta x^2 + \Delta y^2} \\ \alpha &= tan^{-1}\left(\frac{F_y(q)}{F_x(q)}\right) - \theta \\ \beta &= -\theta - \alpha \end{aligned} \tag{9}$$

If the value lies between $\frac{-\pi}{2}$ and $\frac{\pi}{2}$, then the kinematic equation based on the coordinates in the polar plane can be seen in (10).

$$\begin{aligned} \dot{\rho} &= -v\ cos\ \alpha \\ \dot{\alpha} &= -\omega + \frac{v\ sin\ \alpha}{\rho} \\ \dot{\beta} &= -\frac{v\ sin\ \alpha}{\rho} \end{aligned} \tag{10}$$

If the target is located in front of the robot, the linear control law can be seen in (11).

$$\begin{aligned} v &= k_\rho \rho \\ \alpha &= k_\alpha \alpha + k_\beta \beta \end{aligned} \tag{11}$$

Therefore, equation (11) is substituted for (10) to produce equation (12).

$$\begin{aligned} \dot{\rho} &= -k_\rho cos\ \alpha \\ \dot{\alpha} &= k_\rho\ sin\ \alpha - k_\alpha \alpha - k_\beta \beta \\ \dot{\beta} &= -k_\rho\ v\ sin\ \alpha \end{aligned} \tag{12}$$

The closed loop system at (12) is stable as long as the value of $k_\rho > 0$, $k_\beta < 0$, and $k_\alpha - k_\beta > 0$.

C. Environmental Design

This study aims to produce a safe path for the robot to reach the target. Robot design and testing can be done through simulation using various software. One of the robot simulators used for designing and testing robots is Webots [20], [21]. Webots is a free and open source 3D robot simulator from Cyberbotics Ltd. Webots are used for modelling, programming and 3D simulation of a mobile robot. Webots are widely used in academia, industry, and research.

The robot used in this research is E-puck. E-puck is a mobile robot platform with a differential drive type that is widely used in education. Some of the data needed in this research are robot position data, robot heading, and obstacle position. The E-puck hardware specification used for input data is robot radius (L). The robot radius on the E-puck robot is 37 mm. This parameter is used to determine the speed of the right and left wheels accordingly (13).

$$\begin{aligned} v_r &= v + \frac{\omega L}{2R} \\ v_l &= v - \frac{\omega L}{2R} \end{aligned} \tag{13}$$

where R is the instantaneous center of curvature (ICC). Robots that move in curve have a center of curve, which is called the ICC.

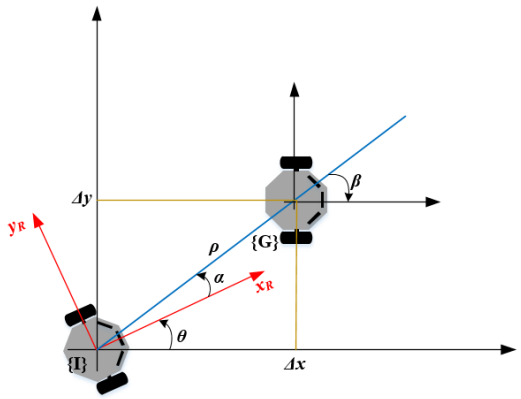

Fig. 2. Kinematics model of WMR

978-1-6654-5412-4/22/$31.00 ©2022 IEEE

The collision-free robot trajectory is obtained from the WMR kinematics equation integrated with the MAPF path planning algorithm. The contribution made to this study was to integrate MAPF into the kinematic model of DDMR. According to Fig. 3, initial position, obstacle, goal, and several gain parameters are input for the path planning algorithm to produce $F_x(q)$ and $F_y(q)$ values. These two parameters are used as input in the WMR kinematics model to produce a collision-free path.

In the simulation, the test area used is 4x4 m, as shown in Fig. 4. The coverage area is -2 to 2 on each x-axis and y-axis. This position is based on the dimensions of the E-puck, which has a radius of 37 mm. In the test environment there are other robots as obstacles. Tests were carried out in both static environments. The static environment is generated from an obstacle in the form of a stationary E-puck robot.

The process of integrating the MAPF algorithm into the DDMR kinematic model can be seen in Fig. 5. Based on Fig. 5, the simulation starts with the initialization of the parameters needed for the path planning algorithm and the kinematic model of DDMR. $F_x(q)$ and $F_y(q)$ values are obtained from the MAPF path planning algorithm. After that, this value is used in the DDMR kinematics model to obtain the value of the robot's position and heading angle. This process will run as long as the robot has not reached the goal.

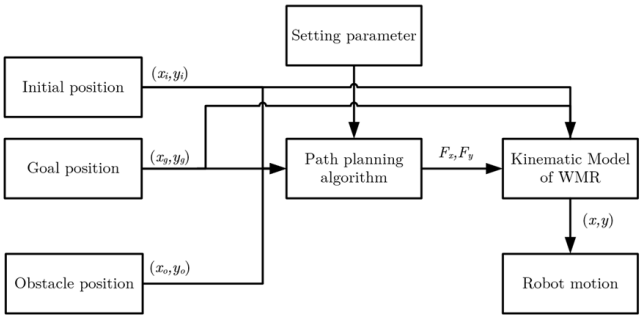

Fig. 3. Block diagram of the system

Fig. 4. Environmental setup

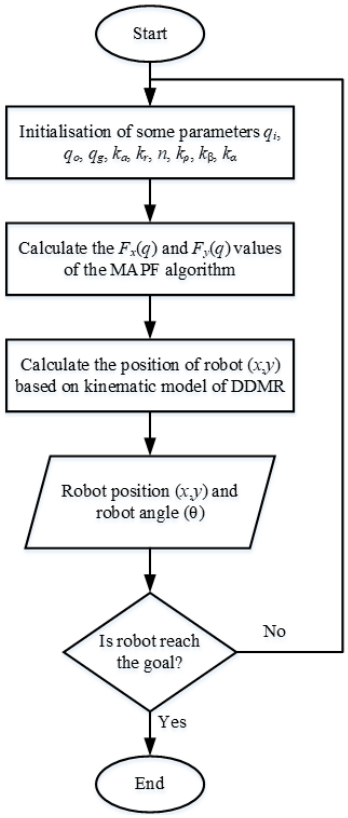

Fig. 5. Flowchart of the system

III. Result and Discussion

A. Effect of Parameter k_α, k_β, k_ρ, and ICC

The effect of parameters k_α, k_β, k_ρ, and ICC can be seen in Fig. 6(a) to (d). According to the test results, k_α and k_β values affect the robot's heading angle, and k_ρ affects the robot's linear speed (11). Based on Fig. 6(a), the k_β and k_ρ values are set to 0.01 and -0.1, respectively. A large k_α value affects producing manoeuvres with small angles. This is shown in the blue line with the value of k_α = 0.13. A small k_α value causes the robot to move farther away. In addition, the broken line at the k_α value of 0.05 indicates that the steps taken from positions q_t and q_{t-1} are quite large.

Fig. 6(b) shows the effect of the value of k_β on the trajectory robot. In this test, the value of k_ρ = 0.01 and k_α= 0.13. A large k_β value affects producing a longer path than a small k_β value. At a small value of k_β, the path generated by the robot goes directly to the goal position. The resulting path length is also smaller than the large k_β value.

Fig. 6(c) shows the effect of the value of k_ρ on the trajectory robot. In this test, the value of k_β = -0.1 and k_α= 0.13. The value of k_ρ affects the linear speed produced by the robot. In this case, a large value of k_ρ affects producing a large step size. If the value of k_ρ is too large, a broken trajectory will occur. This is due to the high speed of the robot in one step.

978-1-6654-5412-4/22/$31.00 ©2022 IEEE

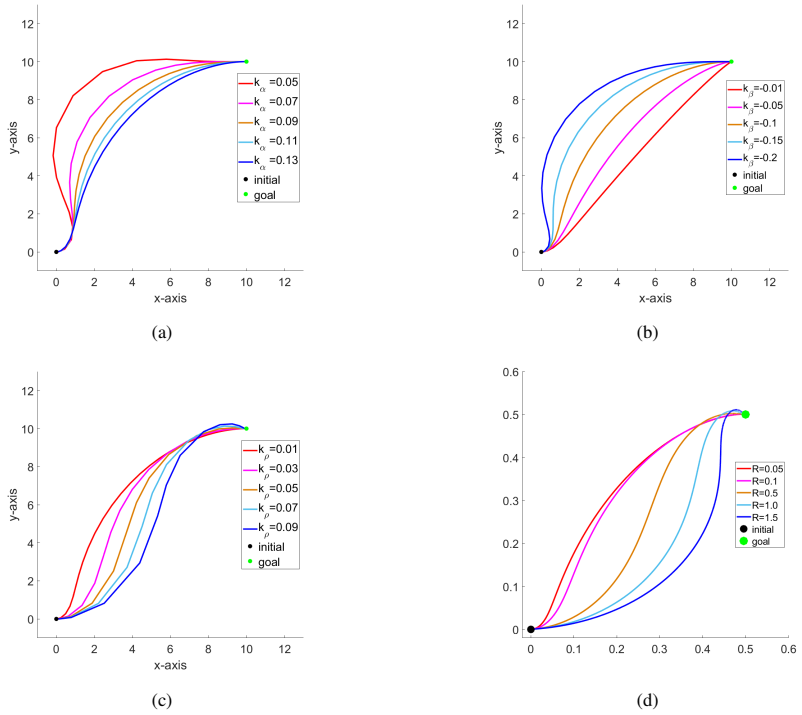

Fig. 6. The effect of some parameters (a) Parameter of k_α (b) Parameter of k_{beta} (c) Parameter of k_ρ (d) Parameter of ICC

TABLE I
PARAMETER OF THE TEST

Environment	Parameter						
	k_a	k_r	k_α	k_β	k_ρ	ICC	n
1	1	50	5	-1	1	0.3	1
2	1	50	5	-1	1	0.3	5

The ICC parameters determine the right (v_r) and left (v_l) motor speeds. The distance from the robot's centre to the curve's centre must be determined properly so that the robot's manoeuvring can also be optimal. Based on Fig. 6(d), a large ICC value causes a longer distance for the robot. The manoeuvre produced by the robot is sharper at a small ICC value. However, the distance to the goal position is getting shorter.

B. Trajectory of Robot

This study uses two tests environment representing the local minimum condition in the form of SAROG and GNRON. In environment 1, the SAROG problem is faced by robots. The obstacle is located symmetrically between the robots and the goal. The initial position of the robot (q_i) is (0,0) with a heading value (θ_i) of 0^0. The obstacle's position (q_o) is located at the coordinates (0.9,0). The goal position (q_g) is located at the coordinates (1.5,0). The parameters used in environment 1 can be seen in Table I.

Based on Fig. 7, the robot managed to avoid a collision and headed for the goal position. The robot stops at the condition $S_{rg} < 0.01$. The distance travelled by the robot is 1.76 m. The

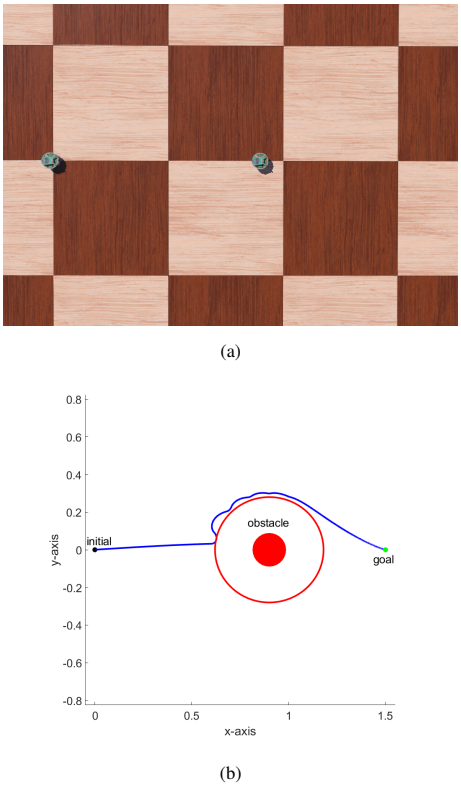

Fig. 7. Trajectory of the robot in environment 1 (a) Representation of environment 1 in Webots (b) Trajectory of robot

978-1-6654-5412-4/22/$31.00 ©2022 IEEE

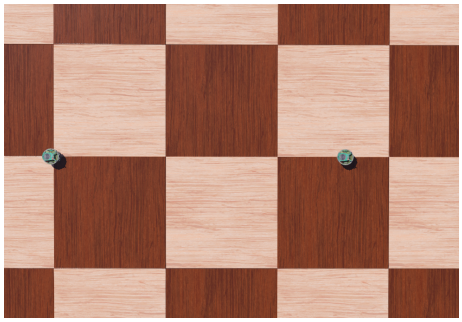

(a)

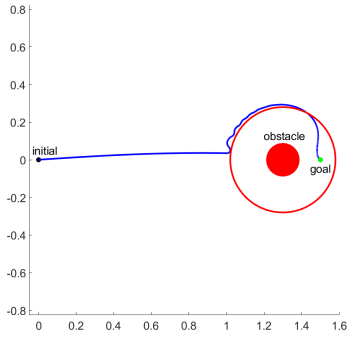

(b)

Fig. 8. Trajectory of the robot in environment 2 (a) Representation of environment 1 in Webots (b) Trajectory of robot

robot's travel time from the initial position to the goal position is 273 s. Based on Fig. 7, the robot can avoid obstacles by performing manoeuvres before reaching the safe limit ($r = 0.3$ m).

Testing on environment 2 represents the GNRON problem. The obstacle is located very close to the goal position. This is indicated by the obstacle which is located at coordinates q_o = (1.3,0). The distance between the obstacle and the goal in the coordinates (1.5,0) is 0.2. This means that the value of $S_{rg} < r$, with a value of r = 0.3. Therefore, according to Table I, the GNRON problem is solved by setting the value of n to 5.

Based on Fig. 8, the robot can avoid obstacles and reach the goal within 317 s. The trajectory generated by the robot falls within the specified safe area. This is a consequence of using Srgn in equation (4). In Fig. 7 and 8, oscillations occur when the robot avoids obstacles. This is caused by determining the parameters that are still less than optimal. However, the robot produced a collision-free trajectory and reached the goal position.

IV. Conclusion

In this study, the MAPF algorithm has been integrated into the WMR kinematics model. The test results show that the trajectory produced by WMR is able to reach the goal and is free of collisions. The Srgn parameter reduces the value of the repulsive potential field generated by obstacles located very close to the goal. However, the gain and ICC parameter settings need to be investigated to reduce robot oscillation when avoiding obstacles.

References

[1] C.-W. Chen, S.-P. Tseng, T.-W. Kuan, and J.-F.Wang, "Outpatient text classification using attention-based bidirectional lstm for robot-assisted servicing in hospital," *Information*, vol. 11, no. 2, 2020.

[2] U. K. Mukherjee and K. K. Sinha, "Robot-assisted surgical care delivery at a hospital: Policies for maximizing clinical outcome benefits and minimizing costs," *Journal of Operations Management*, vol. 66, no. 1-2, pp. 227–256, 2020.

[3] G. Karalekas, S. Vologiannidis, and J. Kalomiros, "Europa: A case study for teaching sensors, data acquisition and robotics via a ros-based educational robot," *Sensors*, vol. 20, no. 9, 2020.

[4] A. Concha Sánchez, J. F. Figueroa-Rodríguez, A. G. Fuentes-Covarrubias, R. Fuentes-Covarrubias, and S. K. Gadi, "Recycling and updating an educational robot manipulator with open-hardware-architecture," *Sensors*, vol. 20, no. 6, 2020.

[5] Y. Luo, S. Li, and D. Li, "Intelligent perception system of robot visual servo for complex industrial environment," *Sensors*, vol. 20, no. 24, 2020.

[6] M. Bottin, S. Cocuzza, N. Comand, and A. Doria, "Modeling and identification of an industrial robot with a selective modal approach," *Applied Sciences*, vol. 10, no. 13, 2020.

[7] L. Emmi, E. Le Flécher, V. Cadenat, and M. Devy, "A hybrid representation of the environment to improve autonomous navigation of mobile robots in agriculture," *Precision Agriculture*, vol. 22, 2021.

[8] A. S. Aguiar, F. N. dos Santos, J. B. Cunha, H. Sobreira, and A. J. Sousa, "Localization and mapping for robots in agriculture and forestry: A survey," *Robotics*, vol. 9, no. 4, 2020.

[9] A. Koubaa et al., "Introduction to Mobile Robot Path Planning," *Studies in Computational Intelligence*, pp. 3–12, 2018, doi: 10.1007/978-3-319-77042-0_1.

[10] S. Yu and Z. Jiang, "Design of the navigation system through the fusion of IMU and wheeled encoders," *Comput. Commun.*, vol. 160, pp. 730–737, 2020.

[11] H. Y. Zhang, W. M. Lin and A. X. Chen, "Path Planning for the mobile robot: A Review", *Symmetry*, vol.10, no.10, pp.450-466, 2018.

[12] X. Fan, Y. Guo, H. Liu, B. Wei and W. Lyu, "Improved articial potential field method applied for AUV path planning", *Mathematical problems in engineering*, pp.1-21, 2020.

[13] M. Guerra, D. Efimov, G. Zheng, andW. Perruquetti, "Avoiding local minima in the potential field method using input-to-state stability," *Control Engineering Practice*, vol. 55, pp. 174–184, 2016.

[14] T. D. Chen and Y. Y. Huang, "Non-trap artificial potential field based on virtual obstacle," *2019 IEEE 16th International Conference on Networking, Sensing and Control (ICNSC)*, 2019, pp. 275–280.

[15] U. Orozco-Rosas, O. Montiel, and R. Sepúlveda, "Mobile robot path planning using membrane evolutionary artificial potential field," *Applied Soft Computing Journal*, vol. 77, pp. 236–251, 2019.

[16] R. D. Puriyanto, O. Wahyunggoro, and A. I. Cahyadi, 'Improved Artificial Potential Field Algorithm Based Multi-Local Minimum Solution', *Eng. Lett.*, vol. 29, no. 3, pp. 1277–1286, 2021.

[17] O. Khatib, "Real-time obstacle avoidance for manipulators and mobile robots," *Proceedings. 1985 IEEE International Conference on Robotics and Automation*, vol. 2, 1985, pp. 500–505.

[18] J. Lee, Y. Nam, and S. Hong, "Random force based algorithm for local minima escape of potential field method," *2010 11th International Conference on Control Automation Robotics Vision*, 2010, pp. 827– 832.

[19] J. Sun, J. U. N. Tang, and S. Lao, "Collision Avoidance for Cooperative UAVs With Optimized Artificial Potential Field Algorithm," *IEEE Access*, vol. 5, pp. 18 382–18 390, 2017.

[20] Y. M. Adam, N. Binti Sariff and N. A. Algeelani, "E-puck Mobile Robot Obstacles Avoidance Controller Using the Fuzzy Logic Approach," *2021 2nd International Conference on Smart Computing and Electronic Enterprise (ICSCEE)*, 2021, pp. 107-112.

[21] S. Rooban, C. Joshitha, I. V. Sai Eshwar and M. s. Latha Gade, "Surveillance and Obstacle Avoiding Autonomous Robot," *2021 Asian Conference on Innovation in Technology (ASIANCON)*, 2021, pp. 1-6.

978-1-6654-5412-4/22/$31.00 ©2022 IEEE